X-ray Emission Studies of the Valence Band of Nanodiamonds Annealed at Different Temperatures

A. V. Okotrub,*,† L. G. Bulusheva,† V. L. Kuznetsov,‡ Yu. V. Butenko,‡ A. L. Chuvilin,‡ and M. I. Heggie§

Institute of Inorganic Chemistry SB RAS, pr. Ak. Lavrentieva 3, Novosibirsk 630090, Russia, Boreskov Institute of Catalysis SB RAS, pr. Ak. Lavrentieva 5, Novosibirsk 630090, Russia, and School of Chemistry, Physics, and Environmental Science, University of Sussex at Brighton, Brighton, U.K.

Received: May 11, 2001; In Final Form: August 6, 2001

X-ray emission spectroscopy has been applied to examine the electronic structure of onion-like carbon (OLC) generated by the annealing treatment of nanodiamonds (ND). The C Kα spectra of OLC produced in the temperature range of 1600−1900 K were found to be markedly different from the spectrum of particles formed at 2140 K and to be characterized by better ordering of graphitic shells. The latter spectrum was shown to be very similar to the C Kα of polycrystalline graphite, while the former ones exhibited a significant increase of the high-energy maximum that might be caused by the defect structure of graphitic networks forming at the intermediate temperatures. The experimental spectra were compared with the theoretical spectra from quantum-chemical semiempirical AM1 calculation of several models: a fullerene molecule, C_{240}, having icosahedral structure, a C_{240} molecule incorporating a greater number of nonhexagonal rings, and a holed structure formed by removing pentagons from the icosahedral molecule. The density of high-energy electronic states in the valence band of the graphitic cage was found to be practically invariant to a change in ring statistics but to significantly increase because of localization of electrons on the zigzag sites of a hole boundary.

Introduction

Carbon is a unique element, yielding the greatest variety of structures involving atoms of one kind only. Carbon structures having nanometer sizes (fullerenes, nanotubes, onions, etc.) presently attract much attention as prospective technological materials, and they constitute a major part of the emerging field of nanotechnology. Fundamental research into these objects is directed toward the link between the topology of the sp^2 carbon network and the properties of the material. Fullerenes and carbon nanotubes are the most widely studied systems (see, for example, refs 1, 2), while still little is known about the electronic states and properties of carbon onions because of significantly lower availability of the samples. Although onion-like carbon (OLC) particles have rather long been detected in arc-discharge products,[3] only after the fullerene discovery did substantial interest in these structures arise. Carbon soot irradiated by intense electron beams was found to reorganize into the quasi-spherical particles composed of concentric graphitic shells.[4] Heat treatment of this soot at temperatures above 2400 K led to the formation of hollow carbon onions.[5] The OLC was also obtained by ion implantation of carbon atoms into a silver substrate heated to 600 °C.[6] Annealing of nanodiamonds (ND) in the temperature range of 1400−1900 K yielded aggregates of OLC particles having up to seven shells.[7] Because this method made it possible to produce onion-containing material in macroscopic quantities, the samples could be studied by various spectroscopic methods: Raman,[8−10] X-ray photoelectron,[11] and electron energy-loss.[12]

The treatment of ND at different temperatures has been found by high-resolution transmission electron microscopy (HRTEM) to generate carbon structures as transient states in the conversion of the diamond particle into a graphite particle.[7] The transformation proceeds from the surface to the center of the diamond particle. At intermediate stages, the particles contain a diamond core coated by graphitic layers, the number of which depends on the transformation depth. During the reorganization of carbon, its density is markedly changed, so graphitic layers in the intermediate structures may be expected to be very defective and characterized by unusual electronic states.

One of the experimental methods for directly probing the electronic structure of molecules and solids is X-ray emission spectroscopy.[13] X-ray emission arises as a result of electron transitions from occupied valence states to a previously created core hole and is governed by the dipole selection rules. Therefore, the C Kα spectrum effectively measures the C 2p partial density of states (dos) in the valence band of a specimen, which can be compared to the same partial dos from quantum-chemical calculations. In the present work, to reveal the electronic state of carbon in the samples produced on the different stages of ND annealing, we have applied the method of ultra-soft X-ray fluorescence spectroscopy. To clarify spectral features, the models of the carbon cage incorporating various defects were calculated using the semiempirical method AM1.

Experiment

The ND samples were prepared by an explosive method and then treated with a hot mixture of concentrated H_2SO_4 and $HClO_4$ acids in a proportion of 1:1 to remove the detonation soot.[14] The annealing of ND samples was performed in a high-vacuum chamber at temperatures of 1170, 1600, 1900, and 2140 K (samples 1, 2, 3, and 4, respectively). The micrographs of the products were obtained with a JEM-2010 transmission electron microscope.

† Institute of Inorganic Chemistry SB RAS.
‡ Boreskov Institute of Catalysis SB RAS.
§ University of Sussex at Brighton.

10.1021/jp011808o CCC: $20.00
Published on Web 09/29/2001

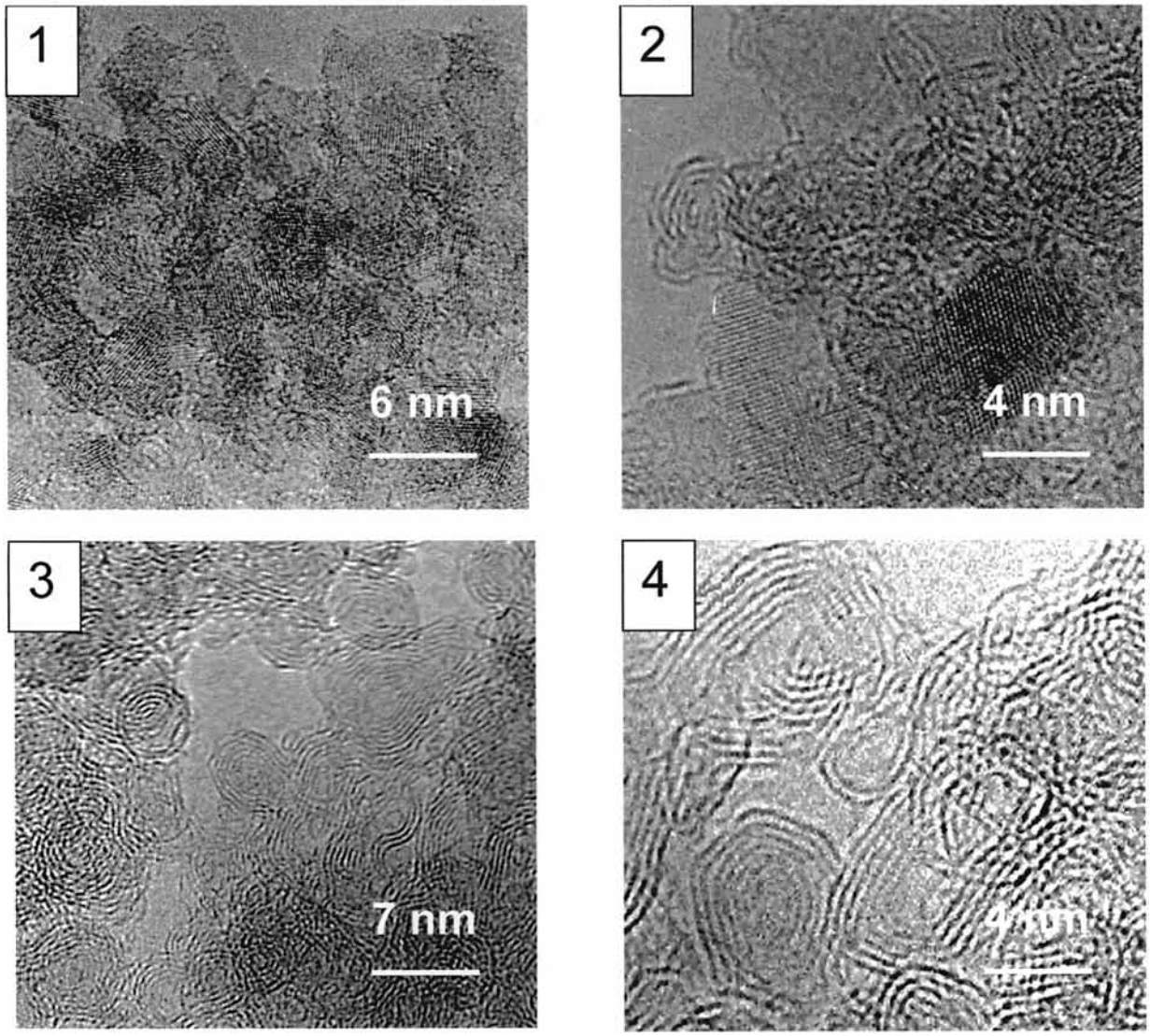

Figure 1. HRTEM images of nanodiamond particles annealed at 1170 K (1), 1600 K (2), 1900 K (3), and 2140 K (4).

X-ray fluorescence spectra of the samples 1−4 and nontextured polycrystalline graphite were recorded with X-ray spectrometer "Stearat" using a crystal analyzer of ammonium biphthalate (NH_4AP). How this crystal is used to obtain the C Kα spectrum is described elsewhere.[15] The samples were deposited on copper supports and cooled to liquid nitrogen temperature in the vacuum chamber of the X-ray tube operating with a copper anode ($U = 6$ kV, $I = 0.5$ A). The nonlinear reflection efficiency of the NH_4AP crystal analyzer allows the reliable measurement of the Kα emission of carbon in the energy region of 285−275 eV. Determination of the X-ray band energy was accurate to ±0.15 eV with spectral resolution of ∼0.5 eV.

Calculation

The quantum-chemical calculations of carbon structures were carried out using the semiempirical AM1 method[16] within the GAMESS package.[17] To model diamond and graphite particles, clusters belonging to T_d and D_{2h} point group symmetries were generated, respectively. The carbon−carbon bonds were assumed to be 1.54 and 1.42 Å long in the diamond and graphite clusters. For saturation of dangling bonds at the cluster boundary, hydrogen atoms were used. The geometries of fullerene molecules of C_{240} composition were fully optimized by the standard BFGS procedure to the gradient value of 10^{-4} Ha/b.

Theoretical C Kα spectra were constructed in the framework of the frozen orbital approximation (Koopman's theorem) on the basis of calculation of the ground state of the compound. X-ray transition intensity was calculated by summing the squared coefficients for carbon 2p atomic orbitals (AOs) in the real occupied molecular orbital (MO). The energy location of intensity corresponded to the MO eigenvalue. Intensities so obtained were normalized by maximal value and broadened by convolution with Lorentzian functions of 0.6 eV half-width at half-maximum (hwhm). To avoid the cluster boundary having an effect on the spectral profile, only the central atoms of diamond and graphite clusters were involved in the calculation.

Results and Discussion

HRTEM Study of the Samples. The HRTEM patterns of the samples under investigation are shown in Figure 1. The sample 1, treated at 1170 K, consists of diamond particles having an average size of 4.7 nm. The distance between the interference fringes, being equal to 2.06 Å, corresponds to the (111) diamond spacing. X-ray photoelectron spectroscopy showed the surface ND particles annealed at this temperature to be free from oxygen.[11] The image of sample 2 demonstrates the rearrangement of the ND surface into graphite layers. In the case of relatively large particles ($d > 3$ nm), the formation of 2−4

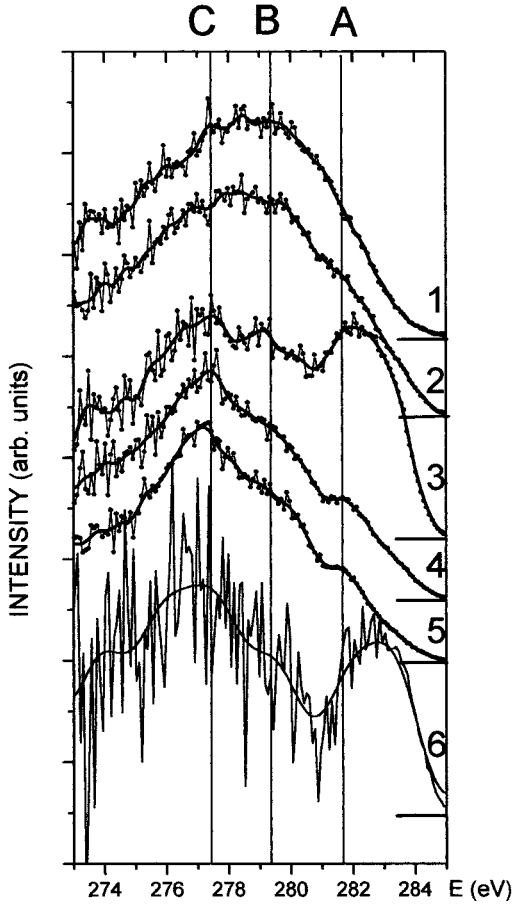

Figure 2. C Kα spectra measured for nanodiamond particles treated at 1170 K (1), 1600 K (2), 1900 K (3), and 2140 K (4) and for non-textured polycrystalline graphite (5). Profile 6 was obtained by subtraction of 0.86 part of the intensity of spectrum 1 from spectrum 2.

graphite-like layers spaced by 0.34−0.35 nm is observed. The proportion of small ND particles having about a 2 nm diameter does not exceed 5%, and such particles are practically completely transformed into graphite ones. The diamond weight fraction in sample 2 has been determined by the measurement of the true density of the sample to be 0.86.[18] Sample 3, prepared at 1900 K, mainly comprises aggregated quasi-spherical OLC particles, which change on further heating above 2140 K to the polyhedral hollow particles (sample 4 depicted in Figure 1). The diamond fraction persists in sample 3 and is 0.15.[18] The core-loss spectrum of spherical carbon onions prepared at similar temperatures also indicated the presence of sp^3-hybridized atoms.[12] In rare cases, a tiny diamond particle residing in the center of a quasi-spherical onion can be detected by electron microscopy.

X-ray Emission Spectra of the Carbon Samples. C Kα spectra of the carbon samples are presented in Figure 2. The spectrum of sample 1 containing ND particles is almost coincident with that of the diamond single crystal.[19] The C Kα spectra of samples 1 and 2 are largely similar in appearance and only exhibit one broad maximum around 279 eV. The spectrum of sample 2 is characterized by a somewhat more pronounced high-energy shoulder, A. The spectrum of sample 4, in which the ND particles are completely transformed into the polyhedral graphitic particles, agrees with the C Kα spectrum of polycrystalline graphite (Figure 2, trace 5). These spectra have the main maximum, C, around 277.5 eV, the high-energy shoulder, B, around 279.2 eV, and the short-wave maximum, A, at 281.6 eV. The C Kα spectrum of sample 4 slightly differs from that of graphite by the location of the main maximum and the relative intensities of marked features. These differences are likely to be caused by contribution of the edge states, of which there are relatively more in the polyhedral particles, which are small in size. The lack of features in the diamond C Kα spectrum comes from the fact that carbon atoms have only σ-type interactions. The electronic structure of graphite comprises σ- and π-states, which can be separated using angle-resolved X-ray spectroscopy.[20] The lines A and C in the spectra of samples 4 and graphite correspond mainly to π- and σ-states, respectively. The feature B is formed by X-ray transitions of both types of electrons. The greatest difference between the spectra of diamond and graphite is observed in the energy region of 278−281 eV and consists of a reduced density of C 2p states in the latter spectrum.

The C Kα spectrum of sample 3, produced at the intermediate temperature, is noticeably different from the spectra of ND particles and of graphitic ones (Figure 2). The spectrum of sample 3 exhibits three maxima at 277.5, 279, and 282 eV. The energy positions of the first two maxima are close to those of the features C and B in the spectrum of sample 4, while the maximum A is shifted by 0.4 eV toward the high-energy spectral region and has surprisingly high intensity (comparable to the intensity of the main maximum). Such enhancement of the maximum A indicates a considerable localization of π electrons, the most probable reason for which is a disruption of the uniformity of the graphite network by defects. Actually, the number of (111) surface atoms of the diamond particle can be estimated and shown to be insufficient to generate an ideal graphitic sphere. The densities of atoms within a fullerene molecule and a (111) diamond face are 2.64 atoms/Å^2 and 2.77 atoms/Å^2, respectively. Considering the increase of layer spacing up to 3.4−3.5 Å in the carbon onion relative to the value of 2.05 Å in diamond, bulk atoms of the ND particle must be involved in the formation of the closed graphitic cage. Because of limited thermal diffusion of carbon atoms at lower temperatures, the graphitic layers developed on the surface of the ND particle might be assumed to be highly defective. The presence of defects and structural irregularities in OLC produced at the intermediate temperatures is strongly supported by the data on the surface area measurements.[18] The surface of OLC particles was detected to increase 1.5−1.6 times compared with that of ND particles, while the estimation from the densities of diamond and ideal graphite (∼1.5) shows this value should be equal to 1.3. When the temperature of ND treatment reaches about 2100 K, the defects in OLC anneal out as indicated by the similarity between the C Kα spectra of sample 4 and graphite. The large cavity (about several nanometers) and the smaller number of layers in the polyhedral particles (Figure 1) suggest that the lack of atoms in graphitic networks is more likely to be compensated by the atoms previously comprising the core and inner shells of OLC particles.

Graphitic layers covering the ND particles and appearing at ∼1600 K could be the cause of the slight distinction of the C Kα spectrum of sample 2 from that of ND particles (sample 1). The X-ray emission spectrum probes the electronic states of all carbon atoms in the sample. For homogeneous materials, such as diamond or graphite, the C Kα spectrum is rather characteristic and corresponds to the density of 2p electronic states of sp^3- or sp^2-hybridized carbon. The C Kα spectrum of sample 2, being a composite, is a superposition of X-ray transitions in at least two kinds of carbon atoms: the first kind constituting the still substantial diamond particle and the second kind involved in graphitic networks. The electronic state of the

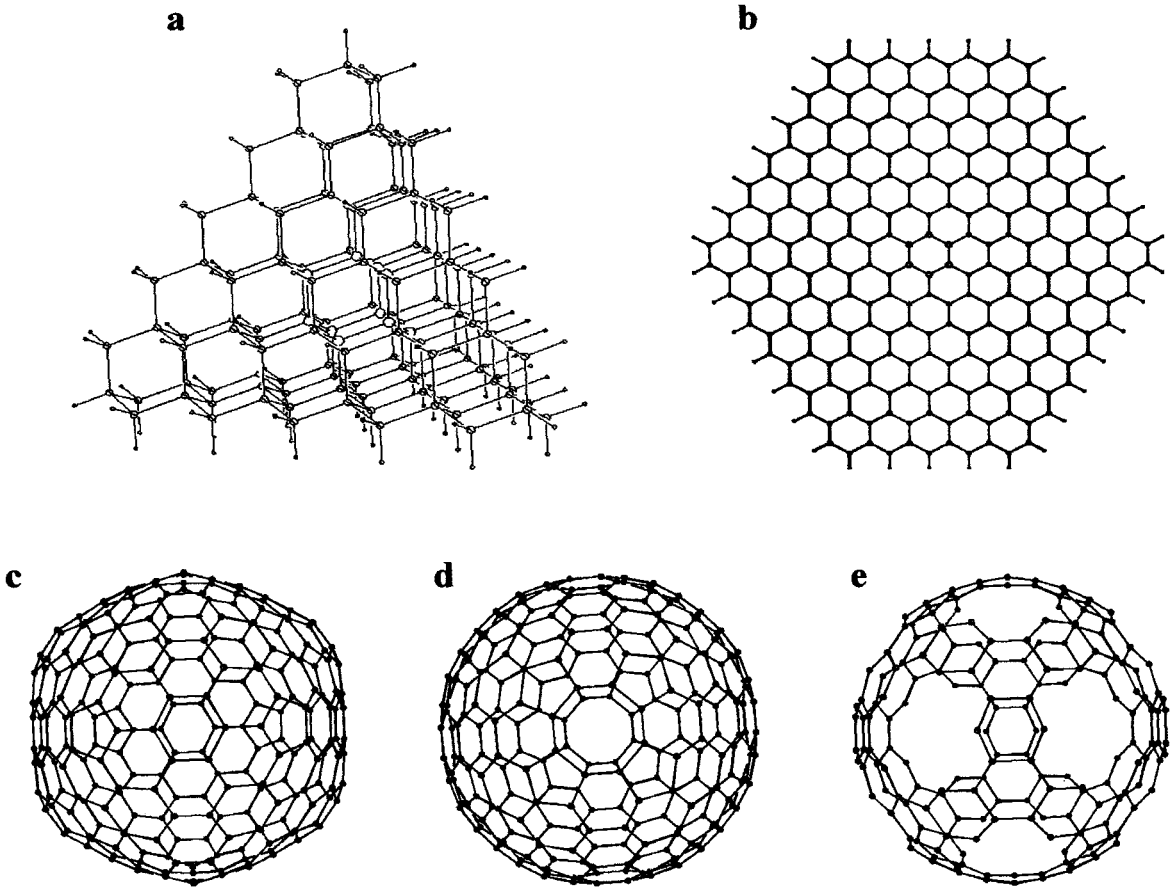

Figure 3. Calculated structures of the hydrogen-terminated diamond fragment $C_{136}H_{104}$ (a), hydrogen-terminated graphite fragment $C_{238}H_{38}$ (b), I_h isomer of C_{240} (c), O_h isomer of C_{240} (d), and holed cage C_{180} (e). Spectra of diamond and graphite were plotted for central atoms.

latter kind of carbon can be revealed by a subtraction of the ND spectrum from the spectrum of sample 2, taking into account the data on the true density of the sample. The spectral profile 6 shown in Figure 2 was obtained by magnifying by a factor 7 the difference between previously normalized intensities of spectrum 2 and a 0.86 part of the intensities of spectrum 1. Summing of the statistical spread in the spectra followed by normalization causes significant reduction in the reliability of the spectral band evaluation. Nevertheless, in the high-energy region characterized by the higher statistics, the maximum at 282.7 eV is evidently detected. The electronic states that formed this maximum are close to the localized π states which appeared in sample 3. The shift of the detected maximum by 0.7 eV toward increasing the X-ray transition energy indicates that corresponding π-states in sample 2 are more weakly bonding than those in sample 3. The small size of graphitic areas generated in sample 2 may be a reason for the energetic shifting of the localized electronic states.

Quantum-Chemical Calculations on Fullerene Cages. To reveal the effect of graphite network topology on the density of occupied 2p electronic states, the quantum-chemical calculations of a number of carbon systems (Figure 3) were performed using AM1 method. The fragments of diamond and graphite consist of 136 and 238 carbon atoms, respectively (Figure 3a,b). The reasonable size of the clusters is expected to substantially reduce the impact of edge electronic states on the spectral profile plotted for the central atoms. The fullerene molecule C_{240} being a second inner shell of the ideal spherical onion[21] was chosen as a model of a closed graphitic cage. Two isomers belonging to I_h and O_h point groups of symmetry were examined. The I_h isomer of C_{240} includes 12 vertexes composed of pentagonal rings (Figure 3c); the O_h isomer of C_{240} contains 24 pentagonal, 92 hexagonal, and 6 octagonal rings and has a more spherical shape (Figure 3d). The ring changes in the carbon cage have been shown to decrease the π delocalization,[22] and it would be of interest to consider the effect of ring statistics on the C Kα spectrum. Finally, the holed cage, C_{180} (Figure 3e), obtained by removing pentagonal rings from the I_h C_{240}, was calculated. The network of this structure comprises conjugated hexagonal rings, some of which incorporate 2-fold coordinated carbon atoms.

Theoretical C Kα spectra for the carbon structures are presented in Figure 4. The energy scale corresponds to the MO eigenvalues calculated for the cage molecules. The spectra modeling the electronic states of diamond (Figure 4a) and graphite (Figure 4b) were aligned to this scale to suit the experimental data from Figure 2. The need for the alignment is caused by the two different types of the calculated structures, those comprising carbon atoms alone and those having a hydrogenated surface. Saturation of the dangling bonds on the edges of diamond and graphite clusters by hydrogen atoms aids iterative convergence during a quantum-chemical calculation. However, the hydrogen atoms induce charge on the carbon cluster that results in equidistant shifting of energy levels. The sifting value may be expected to be dependent on the ratio between bulk and surface atoms in the calculated structure. The relation between the theoretical spectra and the experimental ones indicates the limitations of the computational scheme used. Thus, the spectrum of the diamond cluster exhibits reduced intensity of the line C. The C Kα spectrum of the graphite fragment has three features A, B, and C, of which the energy separations are close to the values in the experimental spectrum

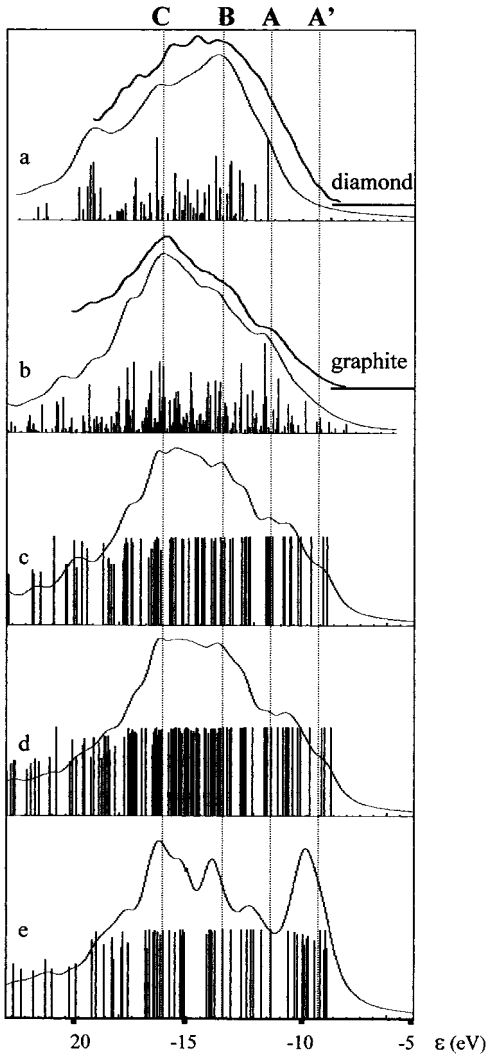

Figure 4. C Kα spectra calculated for diamond cluster $C_{136}H_{104}$ (a), graphite cluster $C_{238}H_{38}$ (b), I_h C_{240} (c), O_h C_{240} (d), and holed cage C_{180} (e). Experimental spectra of nanodiamond particles and polycrystalline graphite are shown for comparison.

but the relative intensities of first two lines are somewhat enhanced. Thus, the calculation on carbon structures provides good fitting to the relative energy of basic features of C Kα spectrum and underestimates the intensity in the long-wave spectral region.

The C Kα spectrum of the icosahedral C_{240} molecule shows the main maximum C and a less intense maximum A (Figure 4c). The shoulders B and A′ are detectable on the high-energy side of these maxima. Relative intensities of the lines B and A′ in the C_{240} spectrum are noticeably higher compared to those in the graphite spectrum. Intensity enhancement is caused by the localization of π electron density in the cage molecule and is more significant for the small cages such as fullerenes C_{60} and C_{70}.[23] Nevertheless, the increase of high-energy intensity of the C_{60} X-ray emission spectrum compared to that of the graphite spectrum[24] is not so crucial because it was fixed for sample 3. The reorganization of electron density due to formation of ideal fullerene-like shells in OLC is not sufficient to fit the features of the latter spectrum. Defects occurring in the graphitic cage can assist the localization of π-state density. The most probable kinds of defect are nonhexagonal rings, sp^3-hybridized atoms, and incomplete bonding.[25] Figure 4d shows the theoretical C Kα spectrum of O_h C_{240} (Figure 3d) incorporating octagons and having twice the number of pentagons of the icosahedral molecule. The comparison between the spectra of these two C_{240} isomers revealed no significant distinctions in the intensity and energy position of the spectral features. The increase of the energy of the highest occupied MO (HOMO) and the number of levels in the interval from −8 to −11 eV indicate the greater localization of π electrons in the O_h symmetric molecule, which, however, is still inadequate to change the C Kα profile significantly. The sp^3 hybridization in OLC, as has been demonstrated by molecular dynamic simulation, may originate from the intershell links.[26] The quantum-chemical calculation of a model constructed from two graphite layers connected by covalent bonds has shown a rather strong change of density of π-electron states relative to that in the graphene sheet.[27] The C Kα spectrum of this calculated model exhibited an increase in the intensity of high-energy features, which is comparable to that in the spectra of C_{240} molecules.

The effect of incomplete bonding in the graphitic shell on the density of occupied states was tested for a C_{180} structure: a three-dimensional network consisting of hexagonal rings only (Figure 3e). The C Kα spectrum plotted for this structure is considerably different from the spectra of other calculated carbon systems especially in the high-energy region (Figure 4). A comparison between the theoretical spectra of graphite and this holed graphitic cage reveals distinctions similar to those observed in the experimental C Kα spectra of polyhedral and spherical particles (Figure 2). The spectrum of the holed structure has three maxima, C, B, and A′. The latter maximum almost reaches the intensity of the main maximum and is shifted from the position of the graphite maximum A by 1.5 eV. A similar shift of the high-energy maximum was detected for the spectral profile 6 of Figure 2, corresponding to the electronic state of graphitic layers generated on the ND surface. The smaller value of energetic shift found in the experiment might be caused by the larger area of the π-conjugated system in the real particles compared with that in the model structure.

One of the reasons for electron density localization may be the formation of zigzag edges in the holed cage. Actually, similar but smaller magnitude effects have been found in the electronic structure of graphene ribbons[28] and carbon nanotube fragments.[29] To analyze in detail C 2p-electron distribution in the valence band of the C_{180} cage, two components assigned to two- and three-coordinated carbon atoms were separated (Figure 5a). The maxima C and B in the C_{180} spectrum correspond mainly to energetic levels occupied by 2p electrons of three-coordinated carbon. The high-energy maximum A′ originates from both types of atoms, but the contribution from electrons of two-coordinated carbon is significantly greater. Calculation of the atomic orbital population indicates that the increase of the maximum at −10 eV is governed by a summing of density of the p_x and p_y electrons of two-coordinated carbon (Figure 5b−d). In the local coordinates, the p_x AO is directed along the dangling C−C bond. The structurally limited overlapping of this component with AOs of neighboring atoms leads to the localization of electrons onto the levels spaced in the narrow interval of ∼1.5 eV (Figure 5b). The p_y component being perpendicular to the surface cage is analogous to the graphite π electron. The energetic splitting of the p_y component in the C_{180} cage is practically the same as that in the icosahedral C_{240}, illustrating the retention of a delocalized π system in the holed structure. However, the occurrence of incomplete bonding restricts the conjugation of π electrons, with the resulting shift of the maximum density in the region of higher energy (Figure 5c). The σ-type interaction of two-coordinated atoms with the

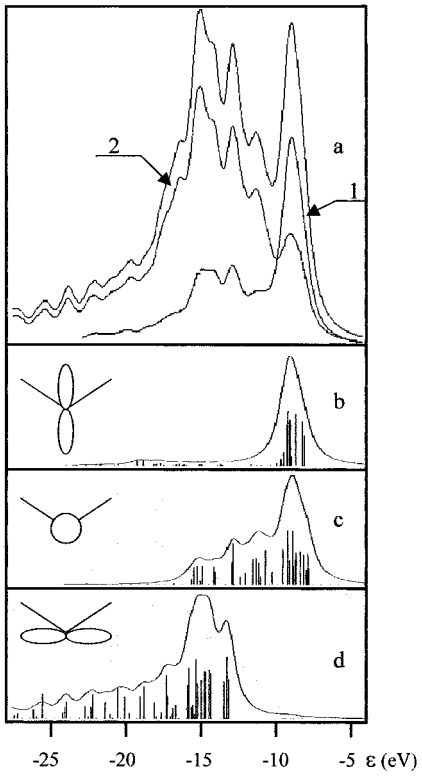

Figure 5. Theoretical C Kα spectrum of C_{180} cage (a) subdivided into two components, corresponding to 2-fold coordinated (line 1) and 3-fold coordinated (line 2) atoms and calculated population of p_x (b), p_y (c), and p_z (d) atomic orbitals of two-coordinated carbon. The direction of these AOs in the local coordinates is schematically shown at the left.

neighbors is realized mainly by the p_z AO (Figure 5d). Tangentially-directed p_x and p_z components could participate in the formation of the same MO, but their mixing is very small as found from the comparison of distributions in Figure 5b,d. The difference in the population of these AOs indicates the loss of equivalency of σ electrons of the two-coordinated carbon atom.

Figure 6 shows examples of the localized MOs, which can be found in the holed graphitic system. The molecular graphs were generated by calculations on a fragment of the C_{180} cage. The change of shading corresponds to the change of wave function phase. The σ-type MO (Figure 6a) is mainly formed by the AOs directed toward the center of the hole. Some overlapping of these orbitals with the AOs of neighboring atoms is the most likely cause of the energetic splitting of the p_x component (Figure 5b). The MO depicted in Figure 6b is characterized by the localization of π-type electrons. Accidental near degeneracy in energy of the localized π states and electron states of the dangling bonds provides the high total density observed in the high-energy region of the holed carbon cage (Figure 5).

Conclusion

Annealing of ND at moderate temperature makes it possible to produce structures that are intermediate in the carbon transformation from the sp^3 to the sp^2 state. Electron microscopy shows that such structures involve cage shells with a spacing close to graphite. However, X-ray emission spectroscopy detects the difference in the electronic state between carbon shells generated below 2140 K and both graphite and diamond particles. An intense maximum found in the high-energy region of the C Kα spectrum indicates significant localization of weakly

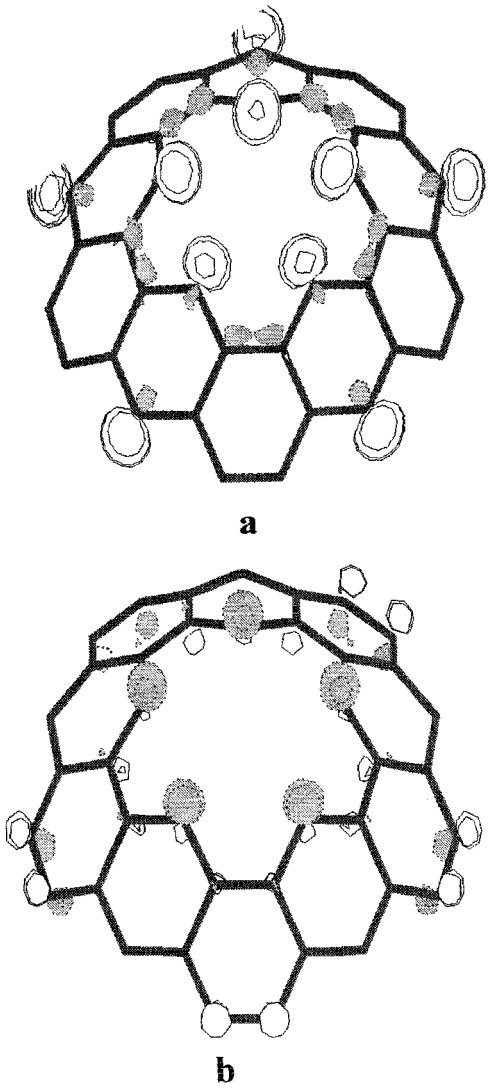

Figure 6. Localized σ- (a) and π-type (b) molecular orbitals in the holed graphitic structure.

bonding electrons in OLC. This localization might result from defects in the curved graphitic networks, namely, the holes which appear through a deficit of surface atoms of ND that are required to form an ideal spherical shell. Quantum-chemical calculation on the holed cage explains the crucial increase of high-energy intensity by the additional contribution of the electrons from dangling bonds on the zigzag edges. The relative chemical inertness of such bonds might be explained by the steric problems occurring when reagents penetrate deep into the OLC through rather small holes.

Acknowledgment. We thank the INTAS (Projects Nos. 97-1700, 00-237), the Russian scientific and technical program ≪Actual directions in physics of condensed states≫ on the ≪Fullerenes and atomic clusters≫ (Project No. 98055) and the Russian Foundation for Basic Research (Project No. 00-03-32463a) for financial support and the Royal Society for a Joint Project grant.

References and Notes

(1) Dresselhaus, M. S.; Dresselhaus, G.; Eklund, P. C. *Science of Fullerenes and Carbon Nanotubes*; Academic Press: London, 1996.

(2) Saito, R.; Dresselhaus, G.; Dresselhaus, M. *Physical Properties of Carbon Nanotubes*; Imperial College Press: London, 1998.

(3) Iijima, S. *J. Cryst. Growth* **1980**, *50*, 675.

(4) Ugarte, D. *Nature (London)* **1992**, *359*, 707.
(5) de Heer, W. A.; Ugarte, D. *Chem. Phys. Lett*. **1993**, *207*, 480.
(6) Cabioc'h, T.; Girard, J. C.; Jaouen, M.; Denanot, M. F.; Hug, G. *Europhys. Lett*. **1997**, *38*, 471.
(7) Kuznetsov, V. L.; Chuvilin, A. L.; Butenko, Yu. V.; Mal'kov, I. Yu.; Titov, V. M. *Chem. Phys. Lett*. **1994**, *222*, 343.
(8) Obraztsova, E. D.; Kuznetsov, V. L.; Loubnin, E. N.; Pimenov, S. M.; Pereverzev, V. G. In *Nanoparticles in Solids and Solutions*; Fendler, J. H., Dekany, I., Eds.; NATO Advanced Study Institute Series 3; Kluwer Academic Publishers: Norwell, MA, 1996; Vol. 18.
(9) Obraztsova, E. D.; Fujii, M.; Hayashi, S.; Kuznetsov, V. L.; Chuvilin, A. L.; Butenko, Yu. V. *Carbon* **1998**, *36*, 821.
(10) Obraztsova, E. D.; Pimenov, S. M.; Konov, V. I.; Fujii, M.; Hayashi, S.; Kuznetsov, V. L.; Butenko, Yu. V.; Chuvilin, A. L.; Loubnin, E. N. *Mol. Mater*. **1998**, *10*, 249.
(11) Kuznetsov, V. L.; Butenko, Yu. V.; Chuvilin, A. L.; Boronin, A. I.; Kvon, R. I.; Kosheev, S. V.; Stankus, S. V.; Khairulin, R. *Ext. Abstr. Program—Bienn. Conf. Carbon* **1997**, *23* (2), 326.
(12) Tomita, S.; Fujii, M.; Hayashi, S.; Yamamoto, K. *Chem. Phys. Lett*. **1999**, *305*, 225.
(13) Urch, D. S. In *Electron Spectroscopy − Theory, Techniques and Application*; Brundle, G. R., Baker, A. D., Eds.; Academic Press Inc.: London, 1979; Vol. 3.
(14) Kuznetsov, V. L.; Malkov, I. Yu.; Chuvilin, A. L.; Moroz, E. M.; Kolomiichuk, V. N.; Shaichutdinov, Sh. K.; Butenko, Yu. V. *Carbon* **1994**, *32*, 873.
(15) Yumatov, V. D.; Okotrub, A. V.; Mazalov, L. N. *Zh. Strukt. Khim*. **1985**, *26*, 59.
(16) Dewar, M. J. S.; Zoebisch, E. S.; Healy, E. F.; Stewart, J. J. P. *J. Am. Chem. Soc*. **1985**, *107*, 3902.
(17) Schmidt, M. W.; Baldridge, K. K.; Boatz, J. A.; Elbert, S. T.; Gordon, M. S.; Jensen, J. H.; Kosoki, S.; Matsunaga, N.; Nguyen, K. A.; Su, S. J.; Windus, T. L.; Dupluis, M.; Montgomery, J. A. *J. Comput. Chem*. **1993**, *14*, 1347.
(18) Butenko, Yu. V.; Kuznetsov, V. L.; Chuvilin, A. L.; Kolomiichuk, V. N.; Stankus, S. V.; Khirulin, R. A.; Segall, B. *J. Appl. Phys*. **2000**, *88*, 4380.
(19) Kurmaev, E. Z.; Shamin, S. N.; Kolobova, K. M.; Shulepov, S. V. *Carbon* **1986**, *24*, 249.
(20) Skytt, P.; Glans, P.; Mancini, D. C.; Guo, J.-H.; Wassdahl, N.; Nordgran, J.; Ma, Y. *Phys. Rev. B* **1994**, *50*, 10457.
(21) Lu, J. P.; Jang, W. *Phys. Rev. B* **1994**, *49*, 11421.
(22) Heggie, M. I.; Terrones, M.; Eggen, B. R.; Jungnickel, G.; Jones, R.; Latham, C. D.; Briddon, P. R.; Terrones, H. *Phys. Rev. B* **1998**, *57*, 13339.
(23) Okotrub, A. V.; Bulusheva, L. G. *Fullerene Sci. Technol*. **1998**, *6*, 405.
(24) Eisebitt, S.; Karl, A.; Eberhardt, W.; Fischer, J. E.; Sathe, C.; Agui, A.; Nordgren, J. *Appl. Phys. A* **1998**, *67*, 89.
(25) Ebbesen, T. W.; Takada, T. *Carbon* **1995**, *33*, 973.
(26) Fugaciu, F.; Hermann, H.; Seifert, G. *Phys. Rev. B* **1999**, *60*, 10711.
(27) Bulusheva, L. G.; Okotrub, A. V.; Asanov, A. V.; Fonseca, A.; Nagy, J. B. *J. Phys. Chem. B* **2001**, *105*, 4853.
(28) Nakada, K.; Fujita, M.; Dresselhaus, G.; Dresselhaus, M. S. *Phys. Rev. B* **1996**, *54*, 17954.
(29) Bulusheva, L. G.; Okotrub, A. V.; Romanov, D. A.; Tomanek, D. *Phys. Low-Dimens. Struct*. **1998**, *3*/*4*, 107.